IEEE Access
Multidisciplinary ⋮ Rapid Review ⋮ Open Access Journal

Received September 9, 2020, accepted October 1, 2020, date of publication October 7, 2020, date of current version October 20, 2020.

*Digital Object Identifier 10.1109/ACCESS.2020.3029227*

# Reactive Current Constraints and Coordinated Control of DFIG's RSC and GSC During Asymmetric Grid Condition

**HAILIANG XU[1], (Member, IEEE), YUFENG ZHANG[1], ZHI LI[1], RENDE ZHAO[1], AND JIABING HU[2], (Senior Member, IEEE)**

[1]College of New Energy, China University of Petroleum (East China), Qingdao 266580, China
[2]School of Electrical and Electronic Engineering, Huazhong University of Science and Technology, Wuhan 430074, China

Corresponding author: Hailiang Xu (xuhl@zju.edu.cn)

This work was supported in part by the National Natural Science Foundation of China under Grant 52077222, and in part by the Fundamental Research Funds for the Central Universities under Grant 19CX02016A.

**ABSTRACT** Doubly fed induction generator (DFIG) based wind turbines have been found to be very sensitive to asymmetrical grid fault, wherein the harmful oscillations in the electromagnetic torque has being made a big concern. What makes things harder is that latest grid codes require grid-connected wind turbines to possess the ability of positive- and negative-sequence reactive current supporting. Hence, it becomes a guide mechanism to meet the grid codes and to ensure the operation safety of the wind turbines. Even though a tradeoff could be made between them, it is still quite difficult to coordinate the current dispatch of the DFIG's rotor- and grid-side converters (RSC and GSC), since there are totally eight currents needing to be carefully designed, i.e., the positive- and negative-sequence active and reactive currents in each converter. To address this issue, this article analyzes the reactive current constraints in detail, based on which a coordinated reactive current control strategy is put forward for the DFIG-based wind turbines during asymmetrical grid condition. Simulation studies demonstrate the effectiveness of the proposed strategy.

**INDEX TERMS** Doubly fed induction generator (DFIG), wind turbine, asymmetrical grid, reactive current support, fault ride-through (FRT).

## I. INTRODUCTION

Nowadays, the doubly fed induction generators (DFIGs) have been widely utilized in wind farms, in virtue of their perfect merits, such as limited converter capacity, wide operating range, high efficiency and reliability [1]–[4]. However, the DFIG-based wind turbine has been found to be quite sensitive to grid disturbance due to the direct connection between the stator windings and the weak power grid [5]. For instance, when an asymmetric grid dip occurs, the DFIG rotor current will get seriously distorted with associated pulsations emerging in the stator active and reactive powers, and the electromagnetic power as well [6]–[9], which may lead to the disconnection of the wind turbines from the faulty grid.

The existing studies focusing on the operation and control of DFIG based wind turbines during asymmetric grid scenario can be divided into two categories, i.e., how to enhance the uninterrupted operation ability of the wind turbines and how to meet the requirement of strict grid codes.

As with the uninterrupted operation (also known as fault ride-through) issue, in [7], it had been revealed that during asymmetric grid fault, the DFIG stator current will be imbalanced, and the rotor current that flowing though the rotor-side converter (RSC) will also be distorted, which could result in the risk of overcurrent. Besides, serious oscillations will emerge in the electromagnetic torque, which threatens the safety of the rotor shafting system [8]. Aiming to enhance the uninterrupted operation ability of the DFIG-based wind turbines, various control methods have been proposed. In [9], a coordinated control of the rotor- and grid-side converters (RSC and GSC, respectively) during voltage unbalance is proposed, where the RSC is controlled to eliminate the torque pulsation at double supply frequency and the GSC is controlled to compensate the oscillation of the stator output

The associate editor coordinating the review of this manuscript and approving it for publication was Seyyed Ali Pourmousavi Kani.

active power. In [10]–[12], it had been found that adopting collaborative control of the RSC and GSC, multiple control targets can be achieved simultaneously. It is noteworthy that in [9]–[12] the harmful torque pulsation is generally recognized to be a big concern in the control improvement of the DFIG system.

With regard to meeting the requirement of grid codes, it is well known that the grid-connected wind turbines should inject positive-sequence reactive current into the faulty grid during symmetrical voltage dips. And the amount of required positive-sequence reactive current is strictly relevant to the degree of positive sequence voltage sag [13]–[15]. In [16], an adaptive reactive current control scheme is proposed to meet the grid code during symmetric fault condition, on the basis of considering both the limit of the GSC and RSC. In [17], an optimized reactive power flow is proposed in the case where an over-excited reactive power support is applied with the joint compensation from both the RSC and the GSC. In [18], a series voltage compensator method is used to reduce considerably the stator and rotor current as well as the rotor voltage, allowing the generator to ride-through the grid disturbances in the light of grid code. Note that the reactive current response methods aforementioned are only capable of dealing with symmetrical grid dips. However, according to statistics, asymmetric grid faults account for about 90% of all grid faults. In fact, with the sustained increase of wind power connected into power grid, grid code starts to put up similar reactive current requirement for wind turbines during asymmetric grid faults [19], [20], which will be named negative-sequence reactive current response in this article. However, few researches have involved this issue. The difficulty lies in two aspects. For the one thing, though various control targets can be achieved as that does in symmetrical grid condition [5], [8], it is difficult to balance the operation safety of the turbines and the reactive current requirement of the grid codes. For the other, given that the control target is reasonably determined, it is still complicated on how to dispatch the positive- and negative-sequence reactive current of the back-to-back converter in the DFIG based system.

To settle such problem, this article puts forward a coordinated control strategy that can simultaneously satisfy the positive- and negative-sequence reactive current requirement by the grid codes and eliminate the harmful oscillations in the electromagnetic torque, with the maximum active power delivery capability being fully considered. The outline of this article is arranged as follows. In Section II, the requirement for both the positive- and negative-sequence reactive current support by the latest grid code is firstly introduced. And the control constraint in eliminating the electromagnetic torque oscillation of the DFIG-based wind turbines is then presented. The detailed current constraints and coordinated control strategy are put forward in Section III. Simulation validations are performed in Section IV. Finally, Section V summarizes some critical conclusions.

## II. CONTROL TARGETS OF THE DFIG-BASED SYSTEM DURING ASYMMETRIC GRID CONDITION

### A. TO SATISFY THE REACTIVE CURRENT REQUIREMENT OF THE GRID CODES

The configuration of the DFIG-based wind turbine is presented in Fig. 1. As shown, the total active and reactive power ($P_t$, $Q_t$) outputted from the wind turbine consist of two parts, i.e., the stator-side active and reactive power ($P_s$, $Q_s$) and the grid-side active and reactive power ($P_g$, $Q_g$), which are controlled by the rotor-side and grid-side converters (RSC and GSC), respectively. Hence, the reactive current response required by the grid codes during asymmetric grid conditions can be satisfied by the coordinated control of the couple of converters.

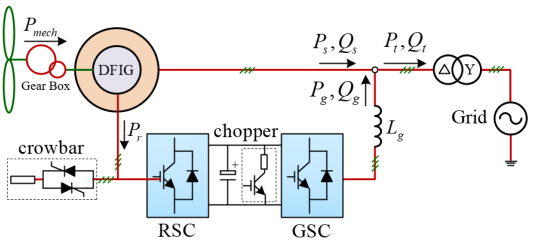


**FIGURE 1.** Configuration diagram of the DFIG-based wind turbine.

According to the latest grid code (revised edition) in China, when the positive sequence component of the grid voltage remains between 47% and 80% of its nominal value, the wind farms should be able to inject certain amount of positive-sequence dynamic reactive current into the grid to support the recovery of the positive-sequence voltage, while absorb given amount of negative-sequence dynamic reactive current from the grid to suppress the rise of the negative-sequence voltage [20]. The detailed reactive current demand in [20] can be summarized as follows:

$$\begin{cases} \Delta i^{+} = K^{+}\left(0.8 - u_{sd+}^{+}\right) I_N \\ \Delta i^{-} = K^{-} u_{sd-}^{-} I_N \end{cases}, \quad 0.47 p.u. \le u_{sd+}^{+} \le 0.8 p.u. \tag{1}$$

where $\Delta i^{+}$, $\Delta i^{-}$ represent the required positive- and negative-sequence reactive current increments, respectively; $K^{+}$ ($\geq 1$), $K^{-}$ ($\geq 1$) denote the positive- and negative-sequence reactive current compensation coefficients, respectively; $u_{sd+}^{+}$, $u_{sd-}^{-}$ represent the remained positive- and negative-sequence voltage components, respectively; $I_N$ is the rated current of the wind turbine.

To give a clear understanding of the gird requirement, Fig. 2 depicts the reactive current response curves of the wind turbines under asymmetric grid fault, when the compensation coefficients $K^{+}$ and $K^{-}$ are both set to be 1. Note that if the compensation coefficients are set larger, more positive- and negative-sequence reactive current increment will be needed.

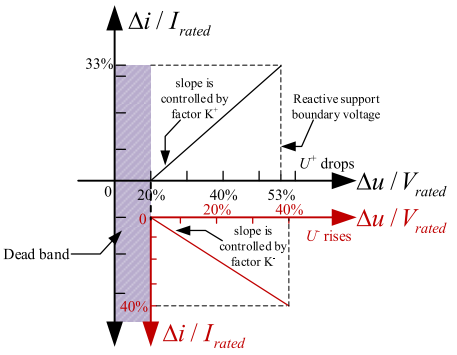


**FIGURE 2.** Reactive current response curves according to the grid code.

### B. TO RESTRAIN THE OSCILLATIONS IN THE ELECTROMAGNETIC TORQUE

As aforementioned, during asymmetric grid condition, the interaction between the positive- and negative-sequence flux and current will produce oscillations in the electromagnetic torque. Detailed derivation can be referred to [8], [21]. Here are given the useful conclusions for analysis convenience.

The T-representation equivalent circuit of a DFIG in the positive synchronous $(dq)^+$ reference frame is shown in Fig. 3.

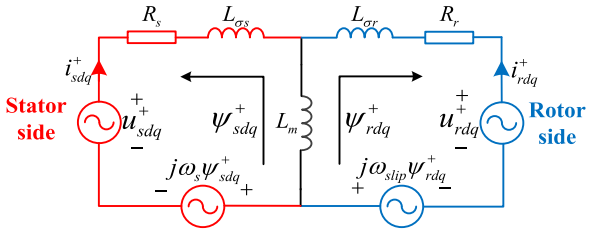


**FIGURE 3.** T-representation of the DFIG equivalent circuit in the positive synchronous reference frame rotating at the speed of $\omega_s$.

According to Fig. 3, the electromagnetic power equals to the sum of the power outputs from the equivalent voltage sources $j\omega_s\,\psi^+_{sdq}$ and $j\omega_{slip}\,\psi^+_{rdq}$, i.e.,

$$\begin{aligned} P_e &= \frac{3}{2}\mathrm{Re}[j\omega_s\psi^+_{sdq}\times\hat{i}^+_{sdq}] + \frac{3}{2}\mathrm{Re}[j\omega_{slip}\psi^+_{rdq}\times\hat{i}^+_{rdq}] \\ &= P_0 + P_{2\omega_s\sin}\sin 2\omega_s t + P_{2\omega_s\cos}\cos 2\omega_s t \end{aligned} \tag{2}$$

where $\omega_r$, $\omega_{slip}$ denote the respective rotor and slip angular frequencies; $\psi^+_{sdq}$, $\psi^+_{rdq}$ represent the respective stator and rotor fluxes, $\hat{i}^+_{sdq}$, $\hat{i}^+_{rdq}$ represent the conjugate of the stator and rotor currents, respectively; $L_s$, $L_m$ denote the stator and mutual inductances, respectively.

Then the electromagnetic torque of the DFIG can be calculated as follows:

$$T_e = \frac{P_e}{\omega_r/p} \tag{3}$$

where $p$ is the number of pole pairs.

Substituting (2) into (3) and decomposing the electromagnetic torque into different pulsating components, yield

$$\begin{aligned} \begin{bmatrix} T_{e,0} \\ T_{e,\sin} \\ T_{e,\cos} \end{bmatrix} &= \frac{3}{2p}\frac{L_m}{L_s}\frac{1}{\omega_s} \\ &\times \begin{bmatrix} -u^+_{sd+} & -u^+_{sq+} & u^-_{sd-} & u^-_{sq-} \\ u^-_{sq-} & -u^-_{sd-} & u^+_{sq+} & -u^+_{sd+} \\ u^-_{sd-} & u^-_{sq-} & -u^+_{sd+} & -u^+_{sq+} \end{bmatrix} \begin{bmatrix} i^+_{rd+} \\ i^+_{rq+} \\ i^-_{rd-} \\ i^-_{rq-} \end{bmatrix} \end{aligned} \tag{4}$$

As represented in (4), under asymmetric grid voltage conditions, the instantaneous electromagnetic torque contains three components, i.e., the DC term, the sine and cosine terms of twice the grid frequency. As a consequence, in order to restrain the oscillations of electromagnetic torque, the sine and cosine terms of twice the grid frequency in (4) should be eliminated, which are related to the positive- and negative-sequence active and reactive rotor currents.

### C. DIFFICULTY IN SIMULTANEOUSLY ACHIEVING THE TWO TARGETS

During asymmetric grid conditions, two control targets, i.e., to meet the grid code and to restrain the oscillations in the electromagnetic torque, have been discussed in detail in the previous sections. In fact, there is another implied target, i.e., outputting active power as much as possible so as to enhance the frequency stability of the grid-connected system. However, such control targets may be contradictory, since they are all related to the controlled currents of the RSC and GSC.

Fig. 4 displays the current coupling constraints in achieving the three aforementioned targets. The complexity can be summarized as follows:

(1) There are too many (totally eight) currents needing to be dispatched and controlled, i.e., the positive- and

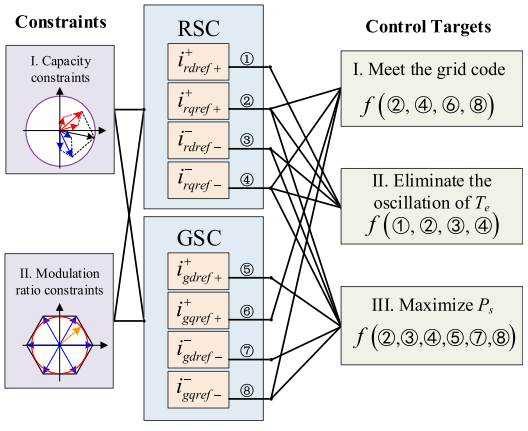


**FIGURE 4.** The coupling constraints in achieving the targets.

negative-sequence active and reactive currents in both the RSC and GSC.

(2) There are complex current couplings in the design of the three control targets, i.e., one current may be related to two or three targets.

(3) There are multiple constraints needing to be concerned simultaneously, i.e., the converters' capacity and modulation constraints, apart from the internal constraints in the control targets I, II and III.

## III. CURRENT REFERENCE ASSIGNMENT AND COORDINATED CONTROL OF THE RSC AND GSC

In order to simultaneously meet the requirements of the grid code and to eliminate the oscillations in the electromagnetic torque, the current references of the RSC and GSC should be carefully dispatched and controlled. Considering that there are totally eight currents needing to be handled, and some of them correlate closely with each other, it is quite necessary to specify the priority in the current dispatching process. In the forthcoming proposed control strategy, the following rules are adopted.

**Rule I**: The positive- and negative-sequence reactive currents required by the grid codes should be set in the top priority. Considering that outputting negative-sequence reactive current from the stator-side will deteriorate the torque oscillation, the negative-sequence reactive current is assigned to be satisfied by the grid-side, while the positive-sequence reactive current is outputted from the stator-side.

**Rule II**: The current references of the RSC should be dispatched and controlled to restrain the oscillations of the electromagnetic torque. Since the positive-sequence reactive current references have been determined by the grid codes, the negative-sequence active and reactive current references can be calculated based on (4).

**Rule III**: The positive-sequence active current should be outputted as much as possible to maintain the grid frequency stability.

When the current references of the RSC and GSC are obtained, the positive- and negative-sequence currents can be controlled respectively with the dual $dq$ control structure, as presented in Fig. 5. The detailed current assignment will be described in the following sections.

### A. CURRENT REFERENCE CONSTRAINTS OF THE RSC

According to the reactive current response requirement, i.e., (1), when the grid voltage is asymmetrically drops, the stator positive-sequence reactive current increment based on Rule I should be set as follows:

$$\Delta i^{+}_{sqref+} = K^{+}\left(0.8 - u^{+}_{sd+}\right) I_N \tag{5}$$

Thus, the total stator positive-sequence reactive current during the LVRT can be obtained as

$$\begin{aligned} i^{+}_{sqref+} &= i^{+}_{sqref0+} + \Delta i^{+}_{sqref+} \\ &= i^{+}_{sqref0+} + K^{+}\left(0.8 - u^{+}_{sd+}\right) I_N \end{aligned} \tag{6}$$

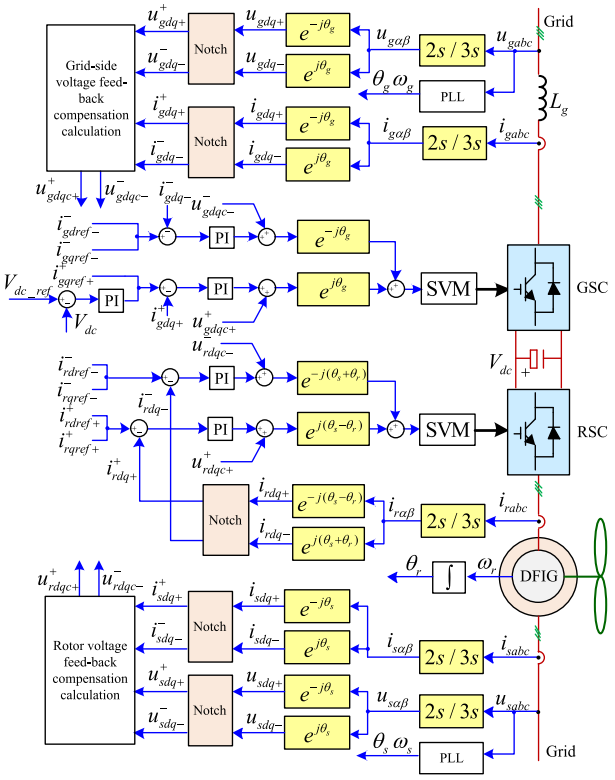


**FIGURE 5.** The control structure of DFIG-based wind turbine.

where $i^{+}_{sqref0+}$ denotes the positive-sequence stator reactive current before the grid fault.

Note that the $q$-axis component of the positive-sequence stator flux can be expressed as

$$\psi^{+}_{sq+} = L_s i^{+}_{sq+} + L_m i^{+}_{rq+} \tag{7}$$

Neglecting the voltage across the stator resistance in Fig. 1, the positive-sequence rotor reactive current reference of the RSC can be obtained as

$$i^{+}_{rq+} = -\frac{u^{+}_{sd+}}{\omega_s L_m} - \frac{L_s}{L_m} i^{+}_{sq+} \tag{8}$$

Assume that the DFIG-based wind turbine was operated in unity power factor (UPF) before the grid fault, i.e., $i^{+}_{sqref0+} = 0$. Then substituting (6) into (8), the positive-sequence reactive rotor current reference can be yielded as

$$i^{+}_{rqref+} = -\left\{u^{+}_{sd+} + \omega_s L_s\left[K^{+}\left(0.8 - u^{+}_{sd+}\right) I_N\right]\right\} / \left(\omega_s L_m\right) \tag{9}$$

As for the negative-sequence rotor current references, according to (4), they can be obtained to eliminate the oscillations of the electromagnetic torque, i.e.,

$$\begin{cases} i^{-}_{rdref-} = k_{sdd} i^{+}_{rdref+} + k_{sqd} i^{+}_{rqref+} \\ i^{-}_{rqref-} = k_{sqd} i^{+}_{rdref+} - k_{sdd} i^{+}_{rqref+} \end{cases} \tag{10}$$

where $k_{sdd} = u^{-}_{sd-}/u^{+}_{sd+}$, $k_{sqd} = u^{-}_{sq-}/u^{+}_{sd+}$.

When the rotor positive-sequence reactive and negative-sequence active and reactive current references, i.e., $i^{+}_{rqref+}$, $i^{-}_{rdref-}$ and $i^{-}_{rqref-}$ are determined, the rotor positive-sequence active current reference, i.e., $i^{+}_{rdref+}$ can be derived based on Rule III. One thing that needs to be considered is the converter's current capacity. Consequently, the settings of the rotor current references should satisfy the following constraint:

$$\sqrt{i^{+2}_{rdref+} + i^{+2}_{rqref+} + i^{-2}_{rdref-} + i^{-2}_{rqref-}} \le I_{r\max} \tag{11}$$

where $I_{r\max}$ represents the maximum current value of the RSC.

When setting up the rotor positive-sequence active current reference, there is another thing needs to be taken account, viz., the available wind power during the LVRT process. Consequently, the rotor positive-sequence active current reference is obtained as

$$i^{+}_{rdref+} = \min\left\{-\frac{2L_s P_{s\max}}{3L_m u^{+}_{sd+}}, \sqrt{\frac{I^2_{r\max} - i^{+2}_{rqref+} - i^{-2}_{rqref-}}{1+k^2_{sdd}}}\right\} \tag{12}$$

where $P_{s\max}$ is the maximum stator active power based on the maximum power point tracking (MPPT) method.

### B. CURRENT REFERENCE CONSTRAINTS OF THE GSC

In response to the negative-sequence reactive current requirement, i.e., (1), during asymmetrically grid voltage drops, the negative-sequence reactive current increment of the GSC should be set as

$$\Delta i^{-}_{gqref-} = K^{-} u^{-}_{gd-} I_N \tag{13}$$

Note that since the DFIG stator windings and the filter inductor of the GSC are connected with the same terminal, as shown in Fig. 1, the negative-sequence reactive current injected from the GSC will affect the stator current, resulting in the deterioration of the electromagnetic torque. So the influence of the negative-sequence reactive current response of the GSC should be considered when realize the goal of Target II.

Thus, the total negative-sequence reactive current during the asymmetrical grid can be obtained as

$$\begin{aligned} i^{-}_{total\_qref-} &= i^{-}_{total\_qref0-} + \Delta i^{-}_{total\_qref-} \\ &= i^{-}_{total\_qref0-} + K^{-} u^{-}_{total\_d-} I_N \end{aligned} \tag{14}$$

where $i^{-}_{total\_qref0-}$ denotes the steady-state value of the total negative-sequence reactive current before the grid fault, $u^{-}_{total\_d-}$ stands for the negative-sequence voltage at PCC.

Note that the $q$-axis component of the negative-sequence stator flux can be expressed as:

$$\psi^{-}_{sq-} = L_s i^{-}_{sq-} + L_m i^{-}_{rq-} \tag{15}$$

Substituting (10) into (15), the negative-sequence reactive power of the PCC injected from the stator-side of DFIG-based wind turbine can be obtained

$$i^{-}_{sq\_osc-} = u^{-}_{sd-}\left(1 + \frac{\omega_s L_m i^{+}_{rqref+}}{u_{sd+}}\right) \Big/ (\omega_s L_s) \tag{16}$$

Subtracting (13) from (16) to obtain the negative-sequence reactive current reference of the GSC, yield

$$\begin{aligned} i^{-}_{gqref-} = K^{-} u^{-}_{total\_d-} I_N - u^{-}_{sd-} \\ \times \left(1 + \frac{\omega_s L_m i^{+}_{rqref+}}{u^{+}_{sd+}}\right) / (\omega_s L_s) \end{aligned} \tag{17}$$

Based on (17), the curves of the negative sequence reactive current of the GSC vs. the positive- and negative-sequence voltage can be obtained, as exhibited in Fig. 6. From the figure, it can be seen that the magnitude of the negative-sequence reactive current of the GSC will increase with the raise of the asymmetry degree.

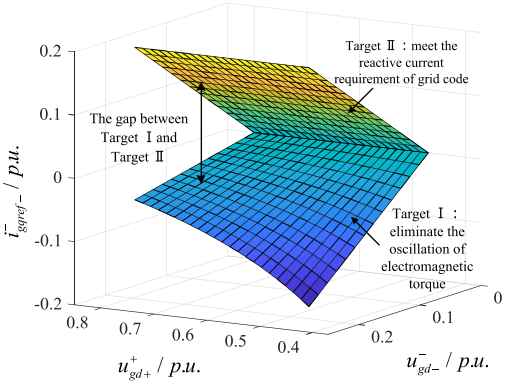


**FIGURE 6.** The curve of negative sequence rotor reactive current limit vs. positive and negative sequence voltage.

Since the positive-sequence reactive current required by the grid code has been provided by the stator side, and the absorption of negative-sequence active current cannot contribute to eliminate the electromagnetic torque oscillation. Therefore, the positive-sequence reactive and negative-sequence active current references can be set as:

$$\begin{cases} i^{+}_{gqref+} = 0 \\ i^{-}_{gdref-} = 0 \end{cases} \tag{18}$$

Then, considering the stator voltage $d$- axis orientation, the active power flowing between GSC and RSC can be expressed as [6]:

$$\begin{aligned} \frac{3L_m s}{2L_s}\left(u^{+}_{sd+} i^{+}_{rdref+} + u^{-}_{sd-} i^{-}_{rdref-}\right) \\ = \frac{3}{2}\left(u^{+}_{gd+} i^{+}_{gdref+} + u^{-}_{gd-} i^{-}_{gdref-}\right) \end{aligned} \tag{19}$$

Based on (19), the positive-sequence active current reference of the GSC can be obtained. Similarly, when the GSC's current capacity is considered, its positive-sequence active

current reference can be finally yielded as

$$i^{+}_{gdref+} = \min \left\{ \begin{array}{l} s\dfrac{L_m}{L_s}\left( i^{+}_{rdref+} + \dfrac{u^{-}_{sd-}}{u^{+}_{sd+}} i^{-}_{rdref-} \right), \\ \sqrt{I^2_{g\max} - i^{+2}_{gqref+} - i^{-2}_{gdref-} - i^{-2}_{gqref-}} \end{array} \right\} \tag{20}$$

where $I_{g\max}$ represents the current limit of GSC.

### C. CONSTRAINTS OF CURRENT REFERENCES CONSIDERING THE PULSE-WIDTH MODULATION

According to the space vector modulation theory, the relations of voltage carrier, modulation wave and modulation ratio at the rotor side should satisfy the following relations:

$$m = \frac{U_{r\max}}{(V_{dc}/2)} \le \frac{2}{\sqrt{3}} \tag{21}$$

where $U_{rmax}$ represents the maximum value of rotor voltage, $V_{dc}$ represents the voltage of DC link.

The positive- and negative-sequence rotor voltage and flux linkage of the DFIG-based wind turbine can be expressed as follows:

$$\begin{cases} u^{+}_{rdq+} = R_r i^{+}_{rdq+} + \dfrac{d\psi^{+}_{rdq+}}{dt} + j\omega_{slip+}\psi^{+}_{rdq+} \\ u^{-}_{rdq-} = R_r i^{-}_{rdq-} + \dfrac{d\psi^{-}_{rdq-}}{dt} + j\omega_{slip-}\psi^{-}_{rdq-} \end{cases} \tag{22}$$

$$\begin{cases} \psi^{+}_{rdq+} = L_r i^{+}_{rdq+} + L_m i^{+}_{sdq+} \\ \psi^{-}_{rdq-} = L_r i^{-}_{rdq-} + L_m i^{-}_{sdq-} \end{cases} \tag{23}$$

where $\omega_{slip+} = \omega_s - \omega_r$, $\omega_{slip-} = -\omega_s - \omega_r$ are the positive- and negative-sequence slip angular frequencies, respectively.

Substituting (22) into (15), and ignoring the little voltage drop on the rotor resistance, yield (24), as shown at the bottom of the page.

According to (23), the positive- and negative-sequence stator current can be expressed as:

$$\begin{cases} i^{+}_{sd+} = -\dfrac{L_m i^{+}_{rd+}}{L_s} \\ i^{+}_{sq+} = \dfrac{u^{+}_{sd+}}{-\omega_s L_s} - \dfrac{L_m i^{+}_{rq+}}{L_s} \\ i^{-}_{sd-} = -\dfrac{L_m i^{-}_{rd-}}{L_s} \\ i^{-}_{sq-} = \dfrac{u^{-}_{sd-}}{\omega_s L_s} - \dfrac{L_m i^{-}_{rq-}}{L_s} \end{cases} \tag{25}$$

Substituting (25) into (24), the RSC constraint considering the modulation constraint can be obtained, i.e.,

$$V_{dc} \ge \sqrt{3}\sqrt{\begin{array}{l} \left(-\omega_{slip+}\sigma L_r i^{+}_{rd+}\right)^2 \\ + \left[\omega_{slip+}\left(\sigma L_r i^{+}_{rq+} - \dfrac{L_m u^{+}_{sd+}}{\omega_s L_s}\right)\right]^2 \\ + \left(-\omega_{slip-}\sigma L_r i^{-}_{rd-}\right)^2 \\ + \left[\omega_{slip-}\left(\sigma L_r i^{-}_{rq-} + \dfrac{L_m u^{-}_{sd-}}{\omega_s L_s}\right)\right]^2 \end{array}} \tag{26}$$

where $\sigma = 1 - \frac{L_m^2}{L_s L_r}$, is the leakage coefficient.

Similarly, the relations of DC link voltage and the positive- and negative-sequence voltage components in the GSC should satisfy the following constraint:

$$V_{dc} \ge \sqrt{3}\sqrt{u^{+2}_{con\_d+} + u^{+2}_{con\_q+} + u^{-2}_{con\_d-} + u^{-2}_{con\_q-}} \tag{27}$$

where $u_{con\_dq}$ represents the $d$- and $q$-axis voltage components of the GSC.

The positive- and negative-sequence voltage equations of the GSC can be expressed as:

$$\begin{cases} u^{+}_{gdq+} = u^{+}_{con\_dq+} + L_g \dfrac{di^{+}_{gdq+}}{dt} + j\omega_g L_g i^{+}_{gdq+} \\ u^{-}_{gdq-} = u^{-}_{con\_dq-} + L_g \dfrac{di^{-}_{gdq-}}{dt} - j\omega_g L_g i^{-}_{gdq-} \end{cases} \tag{28}$$

Consequently, based on (17), (18), (20) and (27), the current limitation of the GSC considering pulse-width modulation can be obtained in (29), as shown at the bottom of the next page.

### D. COMPREHENSIVE FEASIBLE REGION BASED ON THE CONSTRAINTS OF THE RSC AND GSC

Based on the above analysis, the positive- and negative-sequence active and reactive current references of the RSC and GSC can be summarized in (30) and (31), as shown at the bottom of the next page.

According to (30) and (31), the feasible operation region of the DFIG-based wind turbine can be obtained. Since the positive-sequence reactive current and negative-sequence reactive and active current references are set in priority, the feasible region of the RSC can be expressed by the available positive-sequence active current, which depends on the positive- and negative-sequence voltages.

According to the constraint analysis in section A, B and C, the operation boundaries of RSC and GSC can be described by positive-sequence active current under the conditions of their own capacity constraint and modulation constraint, which are determined by the positive- and negative-sequence

$$V_{dc} \ge \sqrt{3}\sqrt{\left(\begin{array}{l} \left[-\omega_{slip+}\left(L_r i^{+}_{rd+} + L_m i^{+}_{sd+}\right)\right]^2 + \left[\omega_{slip+}\left(L_r i^{+}_{rq+} + L_m i^{+}_{sq+}\right)\right]^2 \\ + \left[-\omega_{slip-}\left(L_r i^{-}_{rd-} + L_m i^{-}_{sd-}\right)\right]^2 + \left[\omega_{slip-}\left(L_r i^{-}_{rq-} + L_m i^{-}_{sq-}\right)\right]^2 \end{array}\right)} \tag{24}$$

voltages, respectively. Nevertheless, in order to depict the feasible region of the whole DFIG-based wind turbine adopting the coordinated control strategy under the constraint conditions, i.e., capacity- and modulation constraints of the RSC and GSC, positive-sequence active current of RSC is selected to express output maximum deduced by (19), which is related to positive- and negative-sequence voltage. Given that $I_{r\max} = 1.2p.u.$, $I_{g\max} = 0.45p.u.$, the feasible region curve of the whole DFIG-based wind turbine can be obtained in Fig. 7.

To give a clear illustration, the feasible region curve of the DFIG-based wind turbine vs. positive- and negative-sequence voltage can be presented in a dimension-reduction pattern by determining the steady-state operating point, for instance, $u^+_{sd+} = 0.7p.u.$. It is notable that the turbine can operate in a far wider range if only the modulation ratio constraint of GSC is considered, which means that the curve of modulation constraint of GSC doesn't play a critical role in the operation range analysis when negative-sequence voltage ranges from 0-0.5$p.u.$ Hence, the feasible region of coordinated control strategy of DFIG-based wind turbine under the condition of $u^+_{sd+} = 0.7p.u.$ can be obtained, as shown in Fig. 8.

From Figs. 7 and 8, it can be concluded that the maximum value of positive-sequence active current under the three constraints all show a downward trend when the degree of unbalance (i.e., the ratio of negative sequence voltage to positive sequence voltage) increases. When the negative-sequence voltage is less than 0.25p.u., the maximum value of output positive-sequence active current of DFIG-based wind turbine is mainly determined by the modulation constraint of RSC. However, the maximum output value of positive-sequence active current of the DFIG-based wind turbine is switched to be determined by the capacity constraint of GSC when

$$V_{dc} \geq \sqrt{3}\sqrt{\begin{array}{l} u^{+2}_{gd+} + \left(\omega_g L_g s \dfrac{L_m}{L_s} i^+_{rd+}\right)^2 \\ + \left\{u^-_{gd-} - \omega_g L_g u^-_{gd-}\left[K^- I_N - \left(1 + \dfrac{\omega_s L_m i^+_{rqref+}}{u^+_{sd+}}\right)/(\omega_s L_s)\right]\right\}^2 \end{array}} \tag{29}$$

$$\begin{cases} i^+_{rdref+} = \begin{cases} \sqrt{\dfrac{\left(I_r^2 - i^{+2}_{rqref+} - i^{-2}_{rqref-}\right)}{\left(1 + k^2_{sdd}\right)}}, & 0. \leq u_{sd-} \leq 0.25p.u. \\ \sqrt{\begin{array}{l} \dfrac{V_{dc}^2}{3} - \left[\omega_{slip+}\left(\sigma L_r i^+_{rqref+} - \dfrac{L_m u^+_{sd+}}{\omega_s L_s}\right)\right]^2 \\ - \dfrac{\omega_{slip-}\left(\sigma L_r i^-_{rqref-} + \dfrac{L_m u^-_{sd-}}{\omega_s L_s}\right)}{(\sigma L_r)^2\left(\omega_{slip+} + \omega_{slip-} k_{sdd}\right)^2} \end{array}}, & 0.25p.u. \leq u_{sd-} \leq 0.28p.u. \end{cases} \\ i^+_{rqref+} = -\dfrac{u_{sd+} + \omega_s L_s\left[K^+(0.8 - u_{sd+}) I_N\right]}{\omega_s L_m} \\ i^-_{rdref-} = k_{sdd} i^+_{rdref+} + k_{sqd} i^+_{rqref+} \\ i^-_{rqref-} = k_{sqd} i^+_{rdref+} - k_{sdd} i^+_{rqref+} \end{cases} \tag{30}$$

$$\begin{cases} i^+_{gdref+} = \begin{cases} s\dfrac{L_m}{L_s}\sqrt{\dfrac{I_r^2 - i^{+2}_{rqref+} - i^{-2}_{rqref-}}{1 + k^2_{sdd}}}, & 0 \leq u_{sd-} \leq 0.25p.u. \\ s\dfrac{L_m}{L_s}\sqrt{\begin{array}{l} \dfrac{V_{dc}^2}{3} - \left[\omega_{slip+}\left(\sigma L_r i^+_{rqref+} - \dfrac{L_m u^+_{sd+}}{\omega_s L_s}\right)\right]^2 \\ - \dfrac{\omega_{slip-}\left(\sigma L_r i^-_{rqref-} + \dfrac{L_m u^-_{sd-}}{\omega_s L_s}\right)}{(\sigma L_r)^2\left(\omega_{slip+} + \omega_{slip-} k_{sdd}\right)^2} \end{array}}, & 0.25p.u. \leq u_{sd-} \leq 0.28p.u \end{cases} \\ i^+_{gqref+} = 0 \\ i^-_{gdref-} = 0 \\ i^-_{gqref-} = u_{sd-}\left[K^- I_N - \left(1 + \dfrac{\omega_s L_m i^+_{rqref+}}{u_{sd+}}\right)/(\omega_s L_s)\right] \end{cases} \tag{31}$$

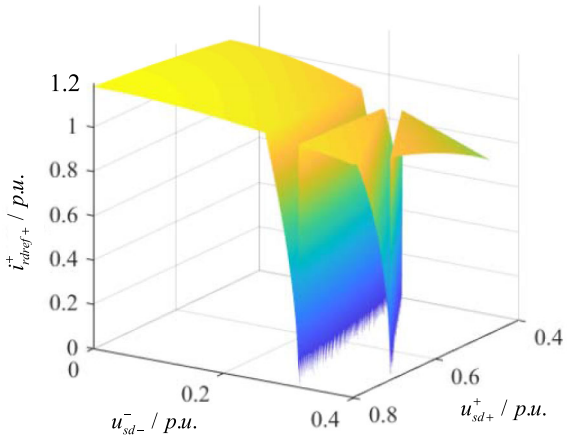


**FIGURE 7.** The feasible region curve of the DFIG-based wind turbine vs. positive- and negative-sequence voltage.

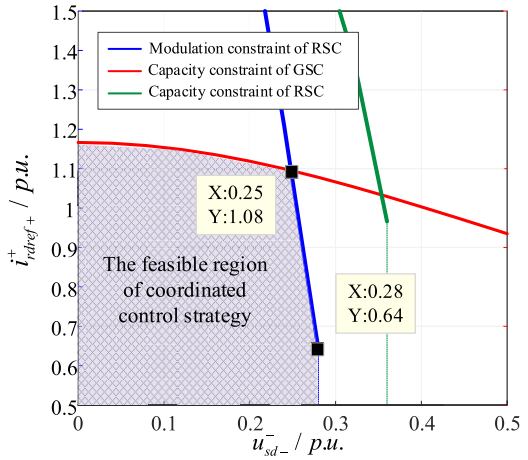


**FIGURE 8.** The feasible region of coordinated control strategy of DFIG-based wind turbine under the condition of $u^+_{sd+} = 0.7p.u.$

the negative-sequence voltage falls between 0.25p.u. and 0.28p.u.

## IV. SIMULATION VERIFICATIONS

To validate the feasibility and effectiveness of the proposed control strategy, simulation tests of a 3MW DFIG-based wind turbine were carried out under the MATLB/Simulink environment. The parameters of the DFIG system are given in Tab. 1.

**TABLE 1.** Parameters of the DFIG system.

| | |
|---|---|
| Grid voltage ($V$) | 690 |
| Grid frequency ($Hz$) | 50 |
| Pole pairs | 3 |
| Stator inductance $L_s$ $(p.u.)$ | 4.229 |
| Rotor inductance $L_r$ $(p.u.)$ | 4.203 |
| Mutual inductance $L_m$ $(p.u.)$ | 3.99 |
| Grid-side filter inductance $L_g$ $(p.u.)$ | 0.65 |

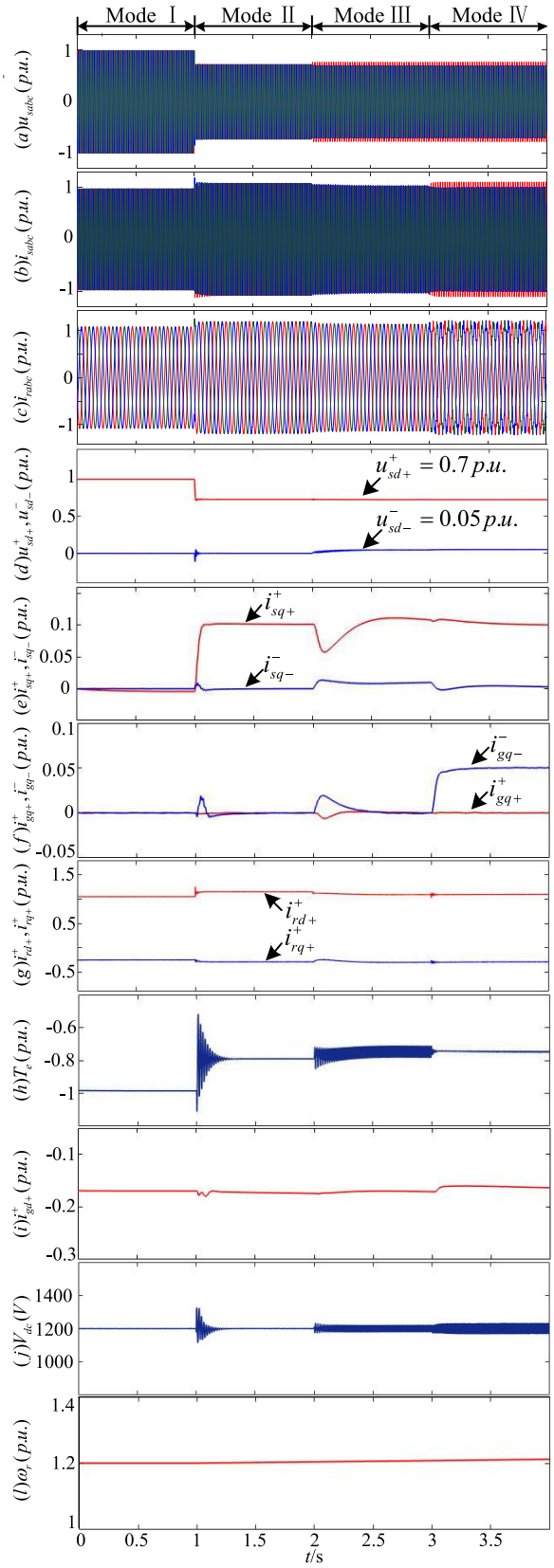


**FIGURE 9.** Simulation results of the DFIG-based wind turbines with different control modes when $u^+_{sd+} = 0.7p.u.$ and $u^-_{sd-} = 0.05p.u.$

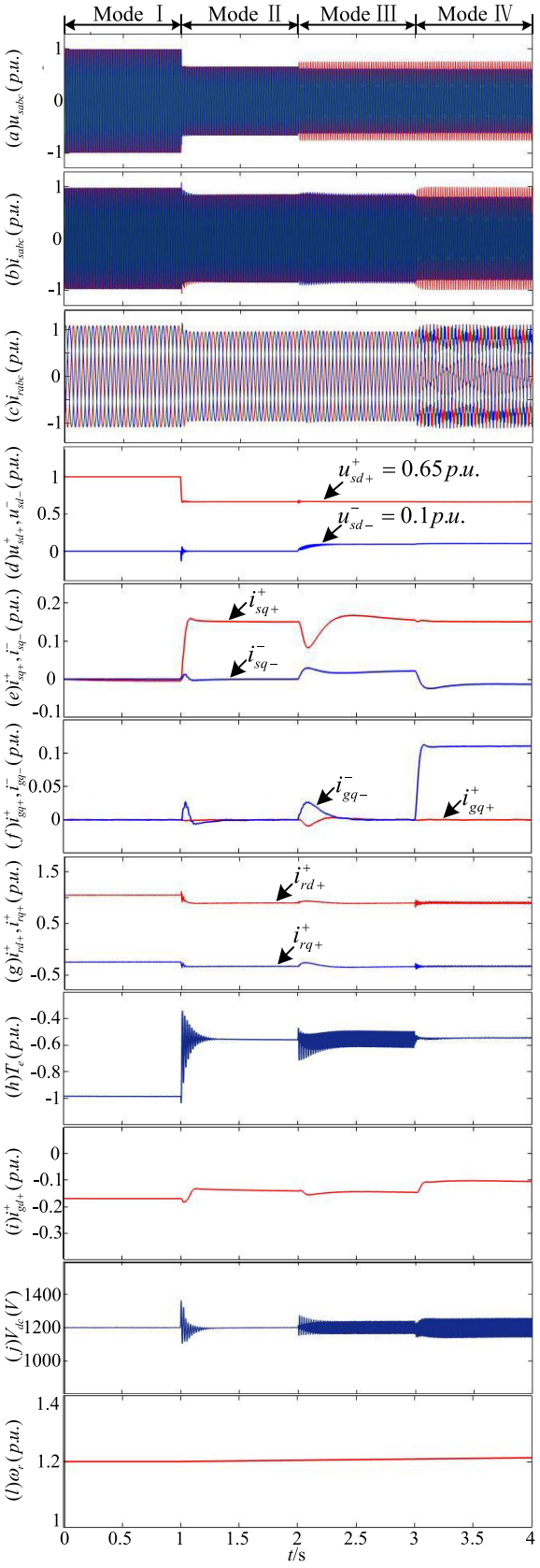


**FIGURE 10.** Simulation results of the DFIG-based wind turbines with different control modes when $u^+_{sd+} = 0.65p.u.$ and $u^-_{sd-} = 0.1p.u.$

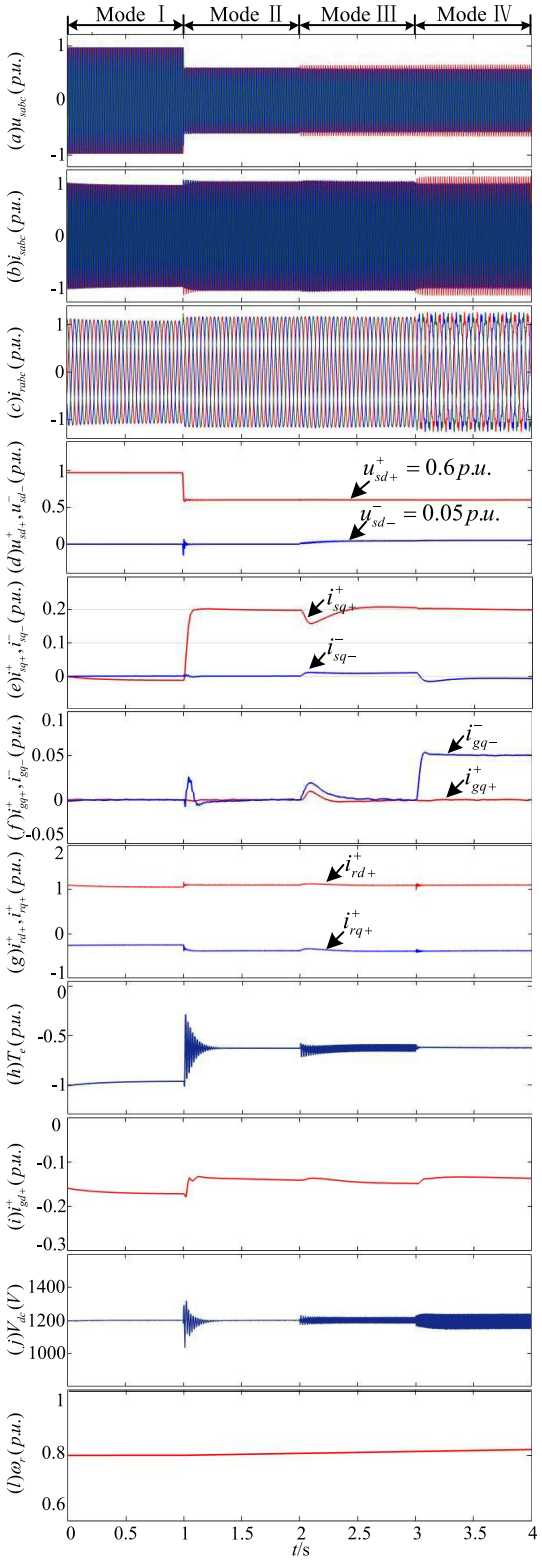


**FIGURE 11.** Simulation results of the DFIG-based wind turbines with different modes in sub-synchronous operation.

The DC-link voltage of the DFIG system is set to be 1200V. And the initial slip ratio is −0.2p.u. The switching

frequencies of the couple of converters are 2.5kHz, while the sampling frequency is 20kHz. Four operation modes are studied during the simulations, i.e., 1) **Mode I**: the grid voltage is normal and the maximum power point tracking control takes in charge; 2) **Mode II**: the grid voltage dips symmetrically, and the positive reactive current response is triggered in accordance with the grid code; 3) **Mode III**: the grid dips asymmetrically, but the control is the same as that in **Mode II**; 4) **Mode IV**: the grid dips asymmetrically, and the proposed positive- and negative- sequence control is adopted. The simulation results are shown in Fig. 9.

As can be seen in Fig. 9, under Mode I, the system is operating approximately at unity power factor. However, when grid voltage sag is detected, the system's operation mode is switched immediately to Mode II, where according to the latest grid code, the DFIG-based wind turbine needs to inject capacitive reactive current of 0.1p.u. into the power network through stator terminator (Fig. 9(e)). Note that the capacitive reactive current is all controlled by the RSC, while the GSC does not participate into the reactive current support, as manifested in Figs. 9 (f) and (i). Thanks to the optimized current assignment, the system keeps uninterruptable operation during this period. When the grid asymmetrical sag appears, the working condition of DFIG system is passively shifted to Mode III, where harmful oscillations begin to emerge in the electromagnetic torque and DC-link voltage, as displayed in Figs. 9(h) and (j), respectively. When the proposed control is triggered, however, the oscillations in the electromagnetic torque can be restrained in a large extent, as shown in Fig. 9(h), while the negative-sequence reactive current requirement is satisfied by the GSC, as depicted in Fig. 9(f).

Further simulations under different grid and operation conditions were conducted, with the waveforms being shown in Figs. 10 and 11, respectively. In Fig. 10, the initial slip ratio is $-0.2$p.u. (super-synchronous), while the positive- and negative-sequence voltages are set as $u^{+}_{sd+} = 0.65p.u.$ and $u^{-}_{sd-} = 0.1p.u.$, respectively. In Fig. 11, the initial slip ratio is 0.2p.u. (sub-synchronous), while the positive- and negative-sequence voltages are set as $u^{+}_{sd+} = 0.6p.u.$ and $u^{-}_{sd-} = 0.05p.u.$, respectively. From the waveforms in Figs. 10 and 11, it can be concluded that during the asymmetrical grid conditions, the oscillations in the electromagnetic torque can be automatically eliminated, while the positive- and negative-sequence current requirement can be satisfied according to the grid codes. The effectiveness and feasibility of the proposed method have also been verified under other operation conditions with similar results obtained, and the waveforms are not shown here due to space limitation.

## V. CONCLUSION

To meet the positive- and negative-sequence reactive current response requirement of the grid codes, the active and reactive current constraints of the DFIG-based wind turbines is derived in this article, based on which a coordinated current assignment strategy of DFIG's RSC and GSC during asymmetric grid conditions is proposed. Some useful conclusions can be summarized as follows.

1) The positive- and negative-sequence reactive currents required by the grid codes should be set in the top priority. Considering that the outputting negative-sequence reactive current from the stator-side will deteriorate the torque oscillations, the negative-sequence reactive current can be assigned to be satisfied by the grid-side (controlled by the GSC), while the positive-sequence reactive current can be delivered from the stator-side (controlled by the RSC).

2) The current references of the RSC can be dispatched in this pattern, i.e., the positive-sequence reactive current reference should be determined by the grid codes, while the negative-sequence active and reactive current references should be set to restrain the oscillation of the electromagnetic torque. Besides, if there is any remained capacity, the positive-sequence active current reference should be set as much as possible to maintain the frequency stability.

3) The current references of the GSC can be arranged in this way, i.e., the negative-sequence reactive current is assigned to meet the requirement of the grid code, and the positive-sequence reactive and negative-sequence active current references can be set to be zero, while the positive-sequence active current rests with the rotor-side positive active current and the capacity of the converter.

4) Based on the proposed current dispatching method, the gird code can be satisfied and the harmful oscillation in the electromagnetic torque can be eliminated as well. Moreover, the boundary of the positive- and negative-sequence reactive and active current references of the couple of converters is presented, which provides a useful guide to dispatch the current references of the DFIG system during such adverse grid condition.

## REFERENCES

[1] R. Cardenas, R. Pena, S. Alepuz, and G. Asher, "Overview of control systems for the operation of DFIGs in wind energy applications," *IEEE Trans. Ind. Electron.*, vol. 60, no. 7, pp. 2776–2798, Jul. 2013.

[2] W. Tang, J. Hu, Y. Chang, and F. Liu, "Modeling of DFIG-based wind turbine for power system transient response analysis in rotor speed control timescale," *IEEE Trans. Power Syst.*, vol. 33, no. 6, pp. 6795–6805, Nov. 2018.

[3] S. Ghosh, Y. J. Isbeih, R. Bhattarai, M. S. E. Moursi, E. F. El-Saadany, and S. Kamalasadan, "A dynamic coordination control architecture for reactive power capability enhancement of the DFIG-based wind power generation," *IEEE Trans. Power Syst.*, vol. 35, no. 4, pp. 3051–3064, Jul. 2020.

[4] J. Hu, Q. Hu, B. Wang, H. Tang, and Y. Chi, "Small signal instability of PLL-synchronized type-4 wind turbines connected to high-impedance AC grid during LVRT," *IEEE Trans. Energy Convers.*, vol. 31, no. 4, pp. 1676–1687, Dec. 2016.

[5] H. Xu, J. Hu, and Y. He, "Operation of wind-turbine-driven DFIG systems under distorted grid voltage conditions: Analysis and experimental validations," *IEEE Trans. Power Electron.*, vol. 27, no. 5, pp. 2354–2366, May 2012.

[6] G. Iwanski, T. Luszczyk, and M. Piwek, "Torque oscillations cancellation targets of a doubly fed induction machine operating with unbalanced and distorted grid," *IEEE Trans. Sustain. Energy*, vol. 11, no. 3, pp. 1636–1646, Jul. 2020.

[7] E. Rezaei, M. Ebrahimi, and A. Tabesh, "Control of DFIG wind power generators in unbalanced microgrids based on instantaneous power theory," *IEEE Trans. Smart Grid*, vol. 8, no. 5, pp. 2278–2286, Sep. 2017.

[8] L. Li, H. Nian, L. Ding, and B. Zhou, "Direct power control of DFIG system without phase-locked loop under unbalanced and harmonically distorted voltage," *IEEE Trans. Energy Convers.*, vol. 33, no. 1, pp. 395–405, Mar. 2018.

[9] A. M. Eltamaly, M. S. Al-Saud, and A. G. Abo-Khalil, "Dynamic control of a DFIG wind power generation system to mitigate unbalanced grid voltage," *IEEE Access*, vol. 8, pp. 39091–39103, 2020.

[10] P. Cheng and H. Nian, "Collaborative control of DFIG system during network unbalance using reduced-order generalized integrators," *IEEE Trans. Energy Convers.*, vol. 30, no. 2, pp. 453–464, Jun. 2015.

[11] G. F. Gontijo, T. C. Tricarico, L. F. D. Silva, D. Krejci, B. W. Franca, M. Aredes, and J. M. Guerrero, "Modeling, control, and experimental verification of a DFIG with a series-grid-side converter with voltage sag, unbalance, and distortion compensation capabilities," *IEEE Trans. Ind. Appl.*, vol. 56, no. 1, pp. 584–600, Jan. 2020.

[12] M. M. Kiani, W. Wang, and W.-J. Lee, "Elimination of system-induced torque pulsations in doubly-fed induction generators via field reconstruction method," *IEEE Trans. Energy Convers.*, vol. 30, no. 3, pp. 1228–1236, Sep. 2015.

[13] M. N. I. Sarkar, L. G. Meegahapola, and M. Datta, "Reactive power management in renewable rich power grids: A review of grid-codes, renewable generators, support devices, control strategies and optimization algorithms," *IEEE Access*, vol. 6, pp. 41458–41489, 2018.

[14] Y.-K. Wu, S.-M. Chang, and P. Mandal, "Grid-connected wind power plants: A survey on the integration requirements in modern grid codes," *IEEE Trans. Ind. Appl.*, vol. 55, no. 6, pp. 5584–5593, Nov. 2019.

[15] M. Dietmannsberger and D. Schulz, "Impacts of low-voltage distribution grid codes on ancillary services and anti-islanding detection of inverter-based generation," *IEEE Trans. Energy Convers.*, vol. 31, no. 4, pp. 1287–1294, Dec. 2016.

[16] H. Xu, X. Ma, and D. Sun, "Reactive current assignment and control for DFIG based wind turbines during grid voltage sag and swell conditions," *J. Power Electron.*, vol. 15, no. 1, pp. 235–245, Jan. 2015.

[17] D. Zhou, F. Blaabjerg, M. Lau, and M. Tonnes, "Optimized reactive power flow of DFIG power converters for better reliability performance considering grid codes," *IEEE Trans. Ind. Electron.*, vol. 62, no. 3, pp. 1552–1562, Mar. 2015.

[18] S. E. da Silveira, S. M. Silva, and B. J. C. Filho, "Fault ride-through enhancement in DFIG with control of stator flux using minimised series voltage compensator," *IET Renew. Power Gener.*, vol. 12, no. 11, pp. 1234–1240, Aug. 2018.

[19] M. A. G. Lopez, J. L. G. D. Vicuna, J. Miret, M. Castilla, and R. Guzman, "Control strategy for grid-connected three-phase inverters during voltage sags to meet grid codes and to maximize power delivery capability," *IEEE Trans. Power Electron.*, vol. 33, no. 11, pp. 9360–9374, Nov. 2018.

[20] *Technical Rule for Connecting Wind Farm to Power System Part One: Onshore Wind Power*, document TC296 GB/T 19963, 2020.

[21] S. Tian, Z. Li, H. Li, Y. Hu, and M. Lu, "Active control method for torsional vibration of DFIG drive chain under asymmetric power grid fault," *IEEE Access*, vol. 8, pp. 155611–155618, 2020.


**HAILIANG XU** (Member, IEEE) received the B.S. degree in electrical engineering from the China University of Petroleum (East China), Qingdao, China, in 2008, and the Ph.D. degree in electrical engineering from Zhejiang University, Hangzhou, China, in 2014.

Since 2018, he has been an Associate Professor with the China University of Petroleum (East China). His current research interests include wind power generation, microgrid, and power quality.

**YUFENG ZHANG** received the B.S. degree from the Luoyang Institute of Science and Technology, Luoyang, China, in 2017. He is currently pursuing the master's degree with the China University of Petroleum (East China). His research interest includes modeling and stability analysis of wind power generation systems.

**ZHI LI** received the B.S. degree from the Shandong University of Science and Technology, Qingdao, China, in 2018. He is currently pursuing the master's degree with the China University of Petroleum (East China). His research interest includes modeling and stability analysis of wind power generation systems.

**RENDE ZHAO** received the B.S. and M.S. degrees in electrical engineering from Shandong University, Jinan, China, in 1999 and 2002, respectively, and the Ph.D. degree from the College of Electrical Engineering, Zhejiang, Hangzhou, China, in 2005.

Since 2006, he has been with the China University of Petroleum (East China), Qingdao, China. He was a Visiting Scholar with Aalborg University, Denmark, from 2015 to 2016. His research interests include renewable energy generation and motor control.

**JIABING HU** (Senior Member, IEEE) received the B.Eng. and Ph.D. degrees from the College of Electrical Engineering, Zhejiang University, Hangzhou, China, in 2004 and 2009, respectively. From 2007 to 2008, he was a Visiting Scholar with the Department of Electronic and Electrical Engineering, University of Strathclyde, Glasgow, U.K., funded by the Chinese Scholarship Council. From April 2010 to August 2011, he was a Postdoctoral Research Associate with the Sheffield Siemens Wind Power Research Center and the Department of Electronic and Electrical Engineering, University of Sheffield, Sheffield, U.K. Since September 2011, he has been a Professor with the State Key Laboratory of Advanced Electromagnetic Engineering and Technology and the School of Electrical and Electronic Engineering, Huazhong University of Science and Technology, Wuhan, China. His current research interests include grid-integration of large-scale renewables; and modeling, analysis, and control of power electronized power systems. He is also a Fellow of the Institute of Engineering and Technology. He is also the Co-Convenor of IEC SC8A JWG5 and an Active Expert of IEC SC8A WG1/AHG3. He was nominated in 2016, 2017, and 2018 by Elsevier to be between the 40 Most Cited Chinese Researchers in electrical and electronic engineering. He serves as an Editor for the IEEE TRANSACTIONS ON ENERGY CONVERSION, an Associate Editor for *IET Renewable Power Generation*, and a member of Editorial Board for *Automation of Electric Power Systems*.